A toolbox for lattice spin models with polar molecules

A. Micheli,* G. K. Brennen, and P. Zoller

Institute for Theoretical Physics, University of Innsbruck,
and Institute for Quantum Optics and Quantum Information of the Austrian Academy of Science, 6020 Innsbruck, Austria
(Dated: October 2, 2018)

There is growing interest to investigate states of matter with topological order, which support excitations in the form of anyons, and which underly topological quantum computing. Examples of such systems include lattice spin models in two dimensions. Here we show that relevant Hamiltonians can be systematically engineered with polar molecules stored in optical lattices, where the spin is represented by a single electron outside a closed shell of a heteronuclear molecule in its rotational ground state. Combining microwave excitation with the dipole-dipole interactions and spin-rotation couplings allows us to build a complete toolbox for effective two-spin interactions with designable range and spatial anisotropy, and with coupling strengths significantly larger than relevant decoherence rates. As an illustration we discuss two models: a 2D square lattice with an energy gap providing for protected quantum memory, and another on stacked triangular lattices leading to topological quantum computing.

I. INTRODUCTION

Lattice spin models are ubiquitous in condensed matter physics where they are used as simplified models to describe the characteristic behavior of more complicated interacting physical systems. Recently there have been exciting theoretical discoveries of models with quasi-local spin interactions with emergent topological order [1, 2]. In contrast to Landau theory where various phases of matter are described by broken symmetries, topological ordered states are distinguished by homology class and have the property of being robust to arbitrary perturbations of the underlying Hamiltonian. These states do not exhibit long range order in pairwise operators, rather they have long range order in highly nonlocal strings of operators. A real world example is the fractional quantum Hall effect which gives rise to states with the same symmetry but distinguishable by quantum numbers associated with the topology of the surface they live on [3].

It is of significant interest to "design" materials with these properties, both to observe and study exotic phases, and in light of possible applications. Cold atomic and molecular gases in optical lattices are prime candidates for this endeavor in view of the complete controllability of these systems in the laboratory. The idea of realizing bosonic and fermionic Hubbard models, and thus also lattice spin models, with cold atoms in optical lattices has sparked a remarkable series of experiments, and has triggered numerous theoretical studies to develop cold atoms as a quantum simulator for strongly correlated condensed matter systems (see e.g. [4, 5, 6] and references therein). However, coaxing a physical system to mimic the required interactions for relevant lattice spin models, which must be both anisotropic in space and in the spin degrees of freedom, and given range, is highly nontrivial. Here we show that cold gases of polar molecules, as presently developed in the laboratory [7], allow us to construct in a natural way a *complete toolbox* for any permutation symmetric two spin-1/2 (qubit) interaction. The attractiveness of this idea

also rests on the fact that dipolar interactions have coupling strengths significantly larger than those of the atomic Hubbard models, and relevant decoherence rates.

Our basic building block is a system of two polar molecules strongly trapped a given sites of an optical lattice, where the spin-1/2 (or qubit) is represented by a single electron outside a closed shell of a heteronuclear molecule in its rotational ground state. Heteronuclear molecules have large permanent electric dipole moments. This implies that the rotational motion of molecules is coupled *strongly* via the dipole-dipole interactions, whose signatures are the *long range* $1/r^3$ character and an *angular dependence*, where the polar molecules attract or repel each other depending on the relative orientation of their dipole moments. In addition, microwave excitation of rotational energy levels allows to effectively tailor the *spatial dependence* of dipole-dipole interactions. Finally, accounting for the spin-rotation splitting of molecular rotational levels we can make these dipole-dipole interactions *spin-dependent*. General lattice spin models are readily built from these binary interactions.

II. ANISOTROPIC SPIN MODELS WITH NOISE RESILIENT GROUND STATES

Two highly anisotropic models with spin-1/2 particles which we will show how to simulate are illustrated in Figs. 1a and 1b respectively. The first takes place on a square 2D lattice with nearest neighbor interactions

$$H_{\mathrm{spin}}^{(\mathrm{I})} = \sum_{i=1}^{\ell-1} \sum_{j=1}^{\ell-1} J(\sigma_{i,j}^z \sigma_{i,j+1}^z + \cos\zeta\, \sigma_{i,j}^x \sigma_{i+1,j}^x). \qquad (1)$$

Introduced by Duoçot *et al.* [8] in the context of Josephson junction arrays, this model (for $\zeta \neq \pm\pi/2$) admits a 2-fold degenerate ground subspace that is immune to local noise up to ℓth order and hence is a good candidate for storing a protected qubit.

The second, occurs on a bipartite lattice constructed with two 2D triangular lattices, one shifted and stacked on top of the other. The interactions are indicated by nearest neighbor
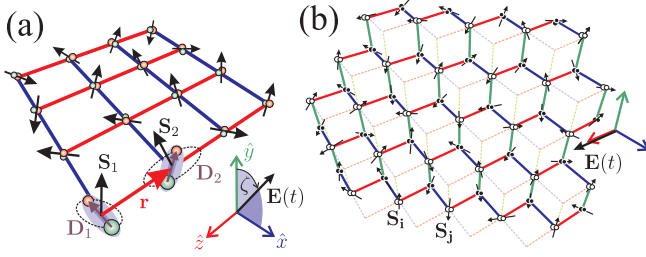
FIG. 1: (Color online) Example anisotropic spin models that can be simulated with polar molecules trapped in optical lattices. (a) Square lattice in 2D with nearest neighbor orientation dependent Ising interactions along $\hat{x}$ and $\hat{z}$. Effective interactions between the spins $\mathbf{S}_1$ and $\mathbf{S}_2$ of the molecules in their rovibrational ground states are generated with a microwave field $\mathbf{E}(t)$ inducing dipole-dipole interactions between the molecules with dipole moments $\mathbf{D}_1$ and $\mathbf{D}_2$, respectively. (b) Two staggered triangular lattices with nearest neighbors oriented along orthogonal triads. The interactions depend on the orientation of the links with respect to the electric field. (Dashed lines are included for perspective.)

links along the $\hat{x}, \hat{y}$ and $\hat{z}$ directions in real space:

$$H_{\text{spin}}^{(\text{II})} = J_\perp \sum_{x-\text{links}} \sigma_j^x \sigma_k^x + J_\perp \sum_{y-\text{links}} \sigma_j^y \sigma_k^y + J_z \sum_{z-\text{links}} \sigma_j^z \sigma_k^z. \quad (2)$$

This model has the same spin dependence and nearest neighbor graph as the model on a honeycomb lattice introduced by Kitaev [9]. He has shown that by tuning the ratio of interaction strengths $|J_\perp|/|J_z|$ one can tune the system from a gapped phase carrying Abelian anyonic excitations to a gapless phase which in the presence of a magnetic field becomes gapped with non-Abelian excitations. In the regime $|J_\perp|/|J_z| \ll 1$ the Hamilonian can be mapped to a model with four body operators on a square lattice with ground states that encode topologically protected quantum memory [10]. One proposal [11] describes how to use trapped atoms in spin dependent optical lattices to simulate the spin model $H_{\text{spin}}^{(\text{II})}$. There the induced spin couplings are obtained via spin dependent collisions in second order tunneling processes. Larger coupling strengths are desirable. In both spin models (I and II) above, the signs of the interactions are irrelevant although we will be able to tune the signs if needed.

III. SPECTROSCOPY OF POLAR MOLECULES IN OPTICAL LATTICES

Our system is comprised of heteronuclear molecules with $^2\Sigma_{1/2}$ ground electronic states, corresponding for example to alkaline-earth monohalogenides with a single electron outside a closed shell. We adopt a model molecule where the rotational excitations are described by the Hamiltonian $H_{\text{m}} = B\mathbf{N}^2 + \gamma\mathbf{N} \cdot \mathbf{S}$ with $\mathbf{N}$ the dimensionless orbital angular momentum of the nuclei, and $\mathbf{S}$ the dimensionless electronic spin (assumed to be $S = 1/2$ in the following). Here B denotes the rotational constant and γ is the spin-rotation coupling constant, where a typical B is a few tens of GHz, and γ in the

hundred MHz regime. The coupled basis of a single molecule i corresponding to the eigenbasis of H_{m}^i is $\{|N_i, S_i, J_i; M_{J_i}\rangle\}$ where $\mathbf{J}_i = \mathbf{N}_i + \mathbf{S}_i$ with eigenvalues $E(N = 0, 1/2, 1/2) = 0, E(1, 1/2, 1/2) = 2B - \gamma$, and $E(1, 1/2, 3/2) = 2B + \gamma/2$. While we ignore hyperfine interactions in the present work, our discussion below is readily extended to include hyperfine effects, which offer extensions to spin systems $S > 1/2$.

The Hamiltonian describing the internal and external dynamics of a pair of molecules trapped in wells of an optical lattice is denoted by $H = H_{\text{in}} + H_{\text{ex}}$. The interaction describing the internal degrees of freedom is $H_{\text{in}} = H_{\text{dd}} + \sum_{i=1}^2 H_{\text{m}}^i$. Here H_{dd} is the dipole-dipole interaction given below in Eq. (3). The Hamiltonian describing the external, or motional, degrees of freedom is $H_{\text{ex}} = \sum_{i=1}^2 \mathbf{P}_i^2/(2m) + V_i(\mathbf{x}_i - \bar{\mathbf{x}}_i)$, where $\mathbf{P}_i$ is the momentum of molecule i with mass m, and the potential generated by the optical lattice $V_i(\mathbf{x} - \bar{\mathbf{x}}_i)$ describes an external confinement of molecule i about a local minimum $\bar{\mathbf{x}}_i$ with 1D rms width z_0. We assume isotropic traps that are approximately harmonic near the trap minimum with a vibrational spacing $\hbar\omega_{\text{osc}}$. Furthermore, we assume that the molecules can be prepared in the motional ground state of each local potential using dissipative electromagnetic pumping [12]. It is convenient to define the quantization axis $\hat{z}$ along the axis connecting the two molecules, $\bar{\mathbf{x}}_2 - \bar{\mathbf{x}}_1 = \Delta z \hat{z}$ with Δz corresponding to a multiple of the lattice spacing.

The near field dipole-dipole interaction between two molecules separated by $\mathbf{r} = \mathbf{x}_1 - \mathbf{x}_2$ is

$$H_{\text{dd}} = \frac{d^2}{r^3} \sum_{q=-1}^1 ((-1)^q D_{1q}^\dagger D_{2-q} - 3D_{10}^\dagger D_{20} + h.c.). \quad (3)$$

The dipole operator coupling the ground and first rotational states of molecule i is $\mathbf{D}_i^\dagger = \sum_{q=-1}^1 |N = 1, q\rangle_{ii}\langle N = 0, 0|\hat{e}_q^*$, and d is the dimensionful dipole moment.

While the present situation of dipole-dipole coupling of rotationally excited polar molecules is reminiscent of the dipole-dipole interaction of between electronically excited atom pairs [13], there are important differences. First, unlike the atomic case where electronically excited states typically are anti-trapped by an optical lattice, here both ground and excited rotational states are trapped by an essentially identical potential. Hence motional decoherence due to spin dependent dipole-dipole forces is strongly suppressed by the large vibrational energy $\hbar\omega_{\text{osc}}$. Second, scattering rates are drastically reduced. The decay rate at room temperature from excited rotational states is $\sim 10^{-3}$ Hz [14] versus a comparable rate of MHz for excited electronic states.

The ground subspace of each molecule is isomorphic to a spin $1/2$ particle. Our goal is to obtain an effective spin-spin interaction between two neighboring molecules. Static spin-spin interactions due to spin-rotation and dipole-dipole couplings do exist but are very small in our model: $H_{\text{vdW}}(r) = -(d^4/2Br^6)\left[1 + (\gamma/4B)^2(1 + 4\mathbf{S}_1 \cdot \mathbf{S}_2/3 - 2S_1^z S_2^z)\right]$. The first term is the familiar van der Waals $1/r^6$ interaction, while the spin dependent piece is strongly suppressed as $\gamma/4B \approx 10^{-3} \ll 1$. Therefore, we propose dynamical mixing with dipole-dipole coupled excited states using a microwave field.

The molecules are assumed trapped with a separation $\Delta z \sim r_\gamma \equiv (2d^2/\gamma)^{1/3}$, where the dipole dipole interaction is $d^2/r_\gamma^3 = \gamma/2$. In this regime the rotation of the molecules is strongly coupled to the spin and the excited states are described by Hunds case (c) states in analogy to the dipole-dipole coupled excited electronic states of two atoms with fine-structure. The ground states are essentially spin independent. In the subspace of one rotational quantum ($N_1 + N_2 = 1$), there are 24 eigenstates of H_{in} which are linear superpositions of two electron spin states and properly symmetrized rotational states of the two molecules. There are several symmetries that reduce H_{in} to block diagonal form. First, H_{dd}, conserves the quantum number $Y = M_N + M_S$ where $M_N = M_{N_1} + M_{N_2}$ and $M_S = M_{S_1} + M_{S_2}$ are the total rotational and spin projections along the intermolecular axis. Second, parity, defined as the interchange of the two molecules followed by parity though the center of each molecule, is conserved. The $\sigma = \pm 1$ eigenvalues of parity are conventionally denoted $g(u)$ for gerade(ungerade). Finally, there is a symmetry associated with reflection R of all electronic and rotational coordinates through a plane containing the intermolecular axis. For $|Y| > 0$ all eigenstates are even under R but for states with zero angular momentum projection there are ± 1 eigenstates of R. The 16 distinct eigenvalues correspond to degenerate subspaces labeled $|Y|_\sigma^\pm(J)$ with J indicating the quantum number in the $r \to \infty$ asymptotic manifold ($N = 0, J = 1/2; N = 1, J$). Remarkably, the eigenvalues and eigenstates can be computing analytically yielding the well known Movre-Pichler potentials [15] plotted in Fig. 2.

IV. ENGINEERING SPIN-SPIN INTERACTIONS

In order to induce strong dipole-dipole coupling we introduce a microwave field $E(\mathbf{x},t)\mathbf{e}_F$ with a frequency ω_F tuned near resonance with the $N = 0 \to N = 1$ transition. Because the rotational states are spaced nonlinearly, this transition is resolvable without coupling to higher rotational states by multiphoton processes. In the rotating wave approximation, the molecule-field interaction is $H_{mf} = -\sum_{i=1}^{2}(\hbar\Omega\mathbf{D}_i^\dagger \cdot \mathbf{e}_F e^{i(\mathbf{k}_F \cdot \mathbf{x}_i - \omega_F t)}/2 + h.c.)$, where the Rabi frequency is $|\Omega| = d|E_0|/\hbar$. As the molecules are trapped by optical wavelengths such that $k_F \Delta z \sim 10^{-5}$ the dipoles are excited in phase only.

The effective Hamiltonian acting on the ground states is obtained in second order perturbation theory as

$$H_{eff}(r) = \sum_{i,f} \sum_{\lambda(r)} \frac{\langle g_f|H_{mf}|\lambda(r)\rangle\langle\lambda(r)|H_{mf}|g_i\rangle}{\hbar\omega_F - E(\lambda(r))}|g_f\rangle\langle g_i|, \quad (4)$$

where $\{|g_i\rangle, |g_f\rangle\}$ are ground states with $N_1 = N_2 = 0$ and $\{|\lambda(r)\rangle\}$ are excited eigenstates of H_{in} with $N_1 + N_2 = 1$ and with excitation energies $\{E(\lambda(r))\}$. The reduced interaction in the subspace of the spin degrees of freedom is then obtained by tracing over the motional degrees of freedom. For molecules trapped in the ground motional states of isotropic harmonic wells with rms width z_0 the wave function is separable in center of mass and relative coordinates with the relative
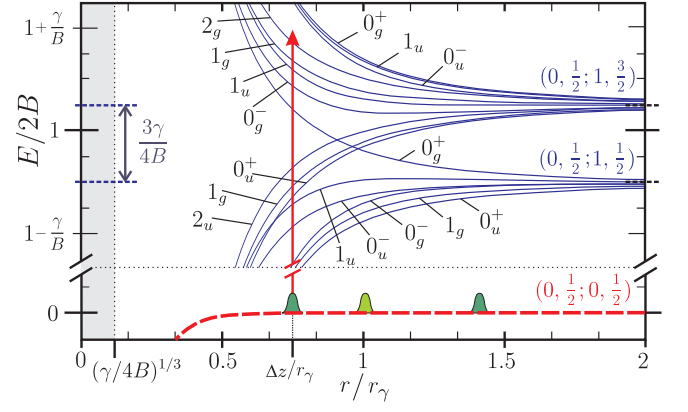

FIG. 2: (Color online) Movre-Pichler potentials for a pair of molecules as a function of their separation r: The potentials $E(g_i(r))$ for the 4 ground-state (dashed lines) and the potentials $E(\lambda(r))$ for the first 24 excited states (solid lines). The symmetries $|Y|_\sigma^\pm$ of the corresponding excited manifolds are indicated, as are the asymptotic manifolds $(N_i, J_i; N_j, J_j)$. The relative coordinate probability densities on a square lattice are depicted on the ground state potential.

coordinate wavefunction

$$\psi_{rel}(r,\theta) = \frac{1}{\pi^{3/4}(2z_0)^{3/2}}e^{-(r^2 + \Delta z^2 - 2r\Delta z \cos\theta)/8z_0^2},$$

where $\cos\theta = \mathbf{r} \cdot \hat{z}/r$. The effective spin-spin Hamiltonian is then $H_{spin} = \langle H_{eff}(r)\rangle_{rel}$.

The Hamiltonian in Eq. (4) is guaranteed to yield some entangling interaction for appropriate choice of field parameters but it is desirable to have a systematic way to design a spin-spin interaction. Fortunately, the model presented here possesses sufficient structure to achieve this essentially analytically. The effective Hamiltonian on molecules 1 and 2 induced by a microwave field is

$$H_{eff}(r) = \frac{\hbar|\Omega|}{8}\sum_{\alpha,\beta=0}^{3}\sigma_1^\alpha A_{\alpha,\beta}(r)\sigma_2^\beta, \quad (5)$$

where $\{\sigma^\alpha\}_{\alpha=0}^3 \equiv \{\mathbf{1}, \sigma^x, \sigma^y, \sigma^z\}$ and A is a real symmetric tensor. See App. A for an explicit form of the matrix coefficients as a function of field polarization and frequency.

Eq. (5) describes a generic permutation symmetric two qubit Hamiltonian. The components $A_{0,s}$ describe a pseudo magnetic field which acts locally on each spin and the components $A_{s,t}$ describe two qubit coupling. The pseudo magnetic field is zero if the microwave field is linearly polarized but a real magnetic field could be used to tune local interactions and, given a large enough gradient, could break the permutation invariance of H_{spin}.

For a given field polarization, tuning the frequency near an excited state induces a particular spin pattern on the ground states. These patterns change as the frequency is tuned though multiple resonances at a fixed intermolecular separation. In Table I it is shown how to simulate the Ising and Heisenberg interactions in this way. Using several fields that are

TABLE I: Some spin patterns that result from Eq. (5). The field polarization is given with respect to the intermolecular axis $\hat{z}$ and the frequency ω_F is chosen to be near resonant with the indicated excited state potential at the internuclear separation Δz. The sign of the interaction will depend on whether the frequency is tuned above or below resonance.

Polarization	Resonance	Spin pattern
$\hat{x}$	2_g	$\sigma^z \sigma^z$
$\hat{z}$	0_u^+	$\vec{\sigma} \cdot \vec{\sigma}$
$\hat{z}$	0_g^-	$\sigma^x \sigma^x + \sigma^y \sigma^y - \sigma^z \sigma^z$
$\hat{y}$	0_g^-	$\sigma^x \sigma^x - \sigma^y \sigma^y + \sigma^z \sigma^z$
$\hat{y}$	0_g^+	$-\sigma^x \sigma^x + \sigma^y \sigma^y + \sigma^z \sigma^z$
$(\hat{y} - \hat{x})/\sqrt{2}$	0_g^+	$-\sigma^x \sigma^y - \sigma^y \sigma^x + \sigma^z \sigma^z$
$\cos\xi \hat{x} + \sin\xi \hat{z}$	1_g	$\lambda_1 (\sigma^x \sigma^z + \sigma^z \sigma^x) + \lambda_2 \sigma^z \sigma^z$ $+ \lambda_3 (\sigma^x \sigma^x + \sigma^y \sigma^y)$
$\cos\xi \hat{y} + \sin\xi \hat{z}$	1_g	$\lambda_1 (\sigma^y \sigma^z + \sigma^z \sigma^y) + \lambda_2 \sigma^z \sigma^z$ $+ \lambda_3 (\sigma^x \sigma^x + \sigma^y \sigma^y)$

sufficiently separated in frequency, the resulting effective interactions are additive creating a *spin texture* on the ground states. The anisotropic spin model $H_{XYZ} = \lambda_x \sigma^x \sigma^x + \lambda_y \sigma^y \sigma^y + \lambda_z \sigma^z \sigma^z$ can be simulated using three fields: one polarized along $\hat{z}$ tuned to $0_u^+(3/2)$, one polarized along $\hat{y}$ tuned to $0_g^-(3/2)$ and one polarized along $\hat{y}$ tuned to $0_g^+(1/2)$. The strengths λ_j can be tuned by adjusting the Rabi frequencies and detunings of the three fields. Using an external magnetic field and six microwave fields with, for example, frequencies and polarizations corresponding to the last six spin patterns in Table I, arbitrary permutation symmetric two qubit interaction are possible.

The effective spin-spin interaction along a different intermolecular axis $\hat{z}'$ can be obtained by a frame transformation in the spherical basis. Writing $\hat{z}' = D^{1\dagger}(\beta_1, \beta_2, \beta_3).(0,1,0)^T$, where D^j is the spin-j Wigner rotation, the effective Hamiltonian along $\hat{z}'$ in the original coordinate system is obtained by the following replacements to the field polarization vector and spin operators: $(\alpha_-, \alpha_0, \alpha_+)^T \rightarrow D^{1\dagger}(\beta_1, \beta_2, \beta_3).(\alpha_-, \alpha_0, \alpha_+)^T$ and $\sigma^\alpha \rightarrow D^{1/2}(\beta_1, \beta_2, \beta_3) \sigma^\alpha D^{1/2\dagger}(\beta_1, \beta_2, \beta_3)$. For example, using a $\hat{z}$ polarized field tuned near $0_u^+(3/2)$ and a field polarized in the $\hat{x} - \hat{y}$ plane tuned near $1_u(3/2)$ creates a Heisenberg interaction between any two molecules separated by **r** with arbitrary orientation in space.

V. APPLICATIONS

We now show how to engineer the spin model I. Consider a system of trapped molecules in a square lattice with site coordinates in the $\hat{z} - \hat{x}$ plane $\{\bar{\mathbf{x}}_{i,j}\} = \{ib\hat{z} + jb\hat{x}; i, j \in [1, \ell] \bigcap \mathbb{Z}\}$. Illuminate the system with a microwave field with linear polarization $\mathbf{e}_F = \cos\zeta \hat{y} + \sin\zeta \hat{x}$ and field frequency ω_F tuned such that the peak of the relative coordinate wavefunction at $r = b$ is near resonant with the 2_g potential but far detuned

from other excited states. Then the dominate interaction between nearest neighbor molecules is of Ising type along each axis and we realize $H_{\mathrm{spin}}^{(I)}$ with $J = (\hbar |\Omega|)^2 \langle 1/8(\hbar \omega_F - 2B - \gamma/2 - d^2/r^3) \rangle_{\mathrm{rel}}$. For realistic parameters, this coupling can range from $10 - 100$ kHz, with the strength constrained by the trap spacing ($J \ll \hbar \omega_{\mathrm{osc}}$). The relative strength of the interactions along $\hat{z}$ and $\hat{x}$ can be changed by rotating the angle ζ of polarization out of plane. Interactions between more distant neighbors are relatively weak because the far off resonant coupling at larger r cannot distinguish the spin dependence of excited states.
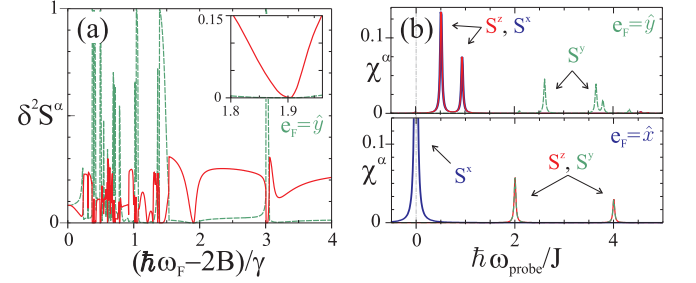

FIG. 3: (Color online) Design and verification of noise protected ground states arising from a simulation of $H_{\mathrm{spin}}^{(I)}$. The system is comprised of 9 polar molecules trapped in a 3×3-square-lattice in the $\hat{z} - \hat{x}$ plane with lattice spacing $b = r_\gamma/\sqrt{2}$ driven with a field of frequency ω_F and out of plane polarization angle ζ. (a) Noise resilience of the ground states of the resultant interaction H_{spin} as a function of field frequency, quantified by the rms-magnetisations of the two ground-states, $\delta^2 S^z = \delta^2 S^x$ (solid-lines) and $\delta^2 S^y$ (dashed lines) for $\zeta = 0$. The inset shows the protected region, when tuning near to the 2_g resonance $E(2_g) \approx 1.9\gamma$ which realizes the model $H_{\mathrm{spin}}^{(I)}$. (b) Absorption-spectroscopy of ground states $\chi^\alpha(\omega_{\mathrm{probe}})$ for two spin-textures obtained by tuning ω_F near the 2_g resonance, $\delta/\gamma = 1.88$, with $b = r_\gamma/\sqrt{2}$. For $\zeta = 0$ the spectrum is gapped by $J/2$, which is a signature of a protected qubit (top), while for $\zeta = \pi/2$ the excitations are gap-less spin-waves (bottom). The peak at $\omega_{\mathrm{probe}} = 0$ is of order unity. The spectroscopic coupling component $\alpha = x, y, z$ (solid,dashed,dotted lines) are indicated.

The authors of Ref. [8] show that the ideal spin model I (for $\zeta \neq \pm\pi/2$) has a 2-fold degenerate ground subspace, which is gapped with weak size dependence for $\cos\zeta = 1$. The the two ground-states, which we denote, $|0\rangle_L$ and $|1\rangle_L$, have zero local magnetizations $\langle \sigma_{i,j}^\alpha \rangle_L$. Our implementation is not ideal because there are residual longer range interactions along several directions in the plane as well as off resonant couplings to excited state potentials yielding unwanted spin patterns. We note, however, that all the effective spin Hamiltonians described in Eq. (5) obtained using fields with linear polarization involve sums of products of Pauli operators and hence are invariant under time-reversal. For ℓ odd, the degeneracy present in the ground state of $H_{\mathrm{spin}}^{(I)}$ is of Kramers' type and imperfect implementation will not break this degeneracy though it may decrease the energy gap.

We have numerically computed the effective interaction on a $\ell^2 = 3 \times 3$ square lattice with spacings $b = r_\gamma/\sqrt{2}$ and we

take the localization to the point dipole limit. In Fig. 3(a) we plot the $\alpha = x, y, z$-components of the rms magnetization for the ground subspace, $\delta^2 S^\alpha \equiv \sum_{ij} \sum_{G'G} |_L\langle G'|\sigma_{i,j}^\alpha|G\rangle_L|^2/2\ell^2$, as a function of the detuning $\omega_F - 2B/\hbar$ for polarization angle $\zeta = 0$. This allows for computing logical qubit errors due to quasi-static noise. Near the bare resonance $\hbar\omega_F - 2B = \gamma/2$ the system show multiple long-range resonances as all the sites couple near-resonantly at coupling strength $\propto 1/b^3$. The last of these long-range resonance appears at $\hbar\omega_F - 2B \approx 1.36\gamma$ for the interaction between next nearest neighbor sites with spacings of $\sqrt{2}b$. The 2_g-resonance lies at $\hbar\omega_F - 2B \approx 1.9\gamma$ for nearest neighbor sites and shows the remarkable feature of no magnetization on any site in any space-direction α withing the ground-state manifold (see inset). The resulting immunity of the system to local noise can be probed by applying an homogeneous B-field of frequency ω_{probe} polarized in the direction $\alpha = x, y, z$. The corresponding absorption spectrum for an arbitrary code state $|\psi\rangle_L$ is, $\chi^\alpha(\omega_{\text{probe}}) \equiv -\hbar\Gamma\Im[_L\langle\psi|S^\alpha(\hbar\omega_{\text{probe}} - H_{\text{spin}} + i\hbar\Gamma)^{-1}S^\alpha|\psi\rangle_L]$ where $S^\alpha = \sum_{ij}\sigma_{i,j}^\alpha/\ell^2$ and Γ is an effective linewidth. This quantity is plotted in Fig. 3(b) for two different spin-textures obtained for the same field frequency $\omega_F = 1.88\gamma$ but different polarizations and were we set $\Gamma = 0.1J$. For polarization $\zeta = 0$ (see top inset) one realizes the protected qubit, whose spectrum is gapped by $J/2$. For polarization along the $\hat{x}$-direction $\zeta = \pi/2$ (see bottom inset) the ground-subspace is given by a set of ℓ quantum-Ising stripes along z, whose spectrum is ungapped with a large peak at $\omega_{\text{probe}} = 0$ in response to coupling with a B field polarized along $\alpha = x$.

Spin model II is likewise obtained using this mechanism. Consider a system of four molecules connected by three length b edges forming an orthogonal triad in space. There are several different microwave field configurations that can be used to realize the interaction $H_{\text{spin}}^{(\text{II})}$ along the links. One choice is to use two microwave fields polarized along $\hat{z}$, one tuned near resonance with a 1_g potential and one near a 1_u potential. When the detunings and Rabi frequencies are chosen so that $\langle|\Omega_{1_g}|C(1_g, 3, 3) - |\Omega_{1_u}|C(1_u, 1, 1)\rangle_{\text{rel}} = 0$ then the resultant spin pattern is Eq. (2) with $J_\perp = -\hbar\langle|\Omega_{1_g}|C(1_g, 3, 3)\rangle_{\text{rel}}/4$ and $J_z = \hbar\langle|\Omega_{1_g}|C(1_g, 2, 2)\rangle_{\text{rel}}/4$. The ratio $|J_\perp|/|J_z|$ can be tuned either by changing the lattice spacing or by using a third microwave field polarized along $\hat{z}$ and tuned near the 2_g potential, in which case $J_\perp \rightarrow J_\perp + \hbar\langle|\Omega_{2_g}|C(2_g)\rangle_{\text{rel}}/8$. A bipartite lattice composed of such triads with equally spaced nearest neighbors can be built using two planes of stacked triangular lattices. Such a lattice could be designed using bichromatic trapping lasers in two spatial dimensions and a suitably modulated lattice in the third dimension normal to both planes. A realization of model II using a different set of 3 microwave fields is shown in Fig. 4. The obtained interaction is close to ideal with small residual coupling to next nearest neighbors as in model I.
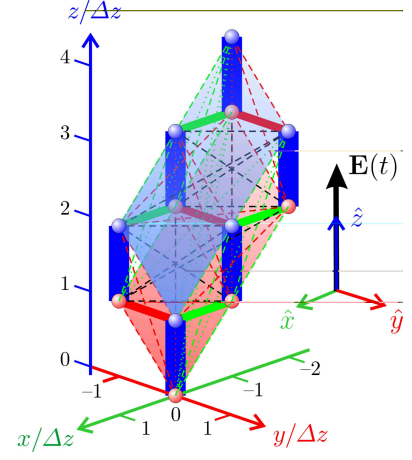

FIG. 4: (Color online) Implementation of spin model $H_{\text{spin}}^{(\text{II})}$. Shown is the spatial configuration of 12 polar molecules trapped by two parallel triangular lattices (indicated by shaded planes) with separation normal to the plane of $\Delta z/\sqrt{3}$ and in plane relative lattice shift of $\Delta z\sqrt{2/3}$. Nearest neighbors are separated by $b = \Delta z$ and next nearest neighbor couplings are at $\sqrt{2}b$. The graph vertices represent spins and the edges correspond to pairwise spin couplings. The edge color indicates the nature of the dominant pairwise coupling for that edge (blue= $\sigma^z\sigma^z$, red= $\sigma^y\sigma^y$, green= $\sigma^x\sigma^x$, black="other"). For nearest neighbor couplings, the edge width indicates the relative strength of the absolute value of the coupling. For this implementation, the nearest neighbor separation is $b = r_\gamma$. Three fields all polarized along $\hat{z}$ were used to generate the effective spin-spin interaction with frequencies and intensities optimized to approximate the ideal model $H_{\text{spin}}^{(\text{II})}$. The field detunings at the nearest neighbor spacing are: $\hbar\omega_1 - E(1_g(1/2)) = -0.05\gamma/2, \hbar\omega_2 - E(0_g^-(1/2)) = 0.05\gamma/2, \hbar\omega_3 - E(2_g(3/2)) = 0.10\gamma/2$ and the amplitudes are $|\Omega_1| = 4|\Omega_2| = |\Omega_3| = 0.01\gamma/\hbar$. For $\gamma = 40$MHz this generates effective coupling strengths $J_z = -100$kHz and $J_\perp = -0.4J_z$. The magnitude of residual nearest neighbor couplings are less than $0.04|J_z|$ along x and y-links and less than $0.003|J_z|$ along z-links. The size of longer range couplings J_{lr} are indicated by edge line style (dashed: $|J_{\text{lr}}| < 0.01|J_z|$, dotted: $|J_{\text{lr}}| < 10^{-3}|J_z|$). Treating pairs of spins on z-links as a single effective spin in the low energy sector, the model approximates Kitaev's 4-local Hamiltonian [10] on a square grid (shown here are one plaquette on the square lattice and a neighbor plaquette on the dual lattice) with an effective coupling strength $J_{\text{eff}} = -(J_\perp/J_z)^4|J_z|/16 \approx 167$Hz.

VI. CONCLUSIONS

We have shown how to engineer pairwise spin-1/2 (or qubit) interactions between polar molecules with designable range and spatial anisotropy. The couplings are strong relative to decoherence rates, and the simulation does not require complicated control sequences to build effective time averaged Hamiltonians, spin-dependent lattices or local addressability. Thus polar molecules in optical lattices are a good candidate to provide a laboratory realization of exotic states of matter. We envision that engineering of these new materials might eventually provide the basis of a new type of quantum optics, where systematic tools are developed which allow the

controlled preparation and manipulation of excitations such as anyons, with applications ranging from fundamental questions in condensed matter physics to quantum computing.

VII. ACKNOWLEDGEMENTS

APPENDIX A: EFFECTIVE INTERACTIONS

The effective spin-spin interaction Eq. (5) between polar molecules depends both on the frequency ω_F and polarization $\mathbf{e}_F = \alpha_- \hat{e}_{-1} + \alpha_0 \hat{e}_0 + \alpha_+ \hat{e}_1$, $(\hat{e}_0 \equiv \hat{z})$ of the field. The explicit form for the coupling coefficients is:

$$
\begin{aligned}
A_{1,1} =\ & |\alpha_0|^2 [C(0_g^-, 1, 2) - C(0_u^+, 1, 2)] \\
& + (|\alpha_-|^2 + |\alpha_+|^2)[C(1_g, 3, 3) - C(1_u, 1, 1)] \\
& + \Re[\alpha_+^* \alpha_-][C(0_g^-, 2, 1) - C(0_g^+, 2, 1)], \\
A_{2,2} =\ & A_{1,1} - 2\Re[\alpha_+^* \alpha_-][C(0_g^-, 2, 1) - C(0_g^+, 2, 1)], \\
A_{3,3} =\ & |\alpha_0|^2 [2C(1_g, 2, 2) - C(0_g^-, 1, 2) - C(0_u^+, 1, 2)] \\
& + (|\alpha_+|^2 + |\alpha_-|^2)[C(2_g) + C(0_g^+, 2, 1)/2 \\
& + C(0_g^-, 2, 1)/2 - C(1_u, 1, 1) - C(1_g, 3, 3)], \\
A_{1,2} =\ & \Im[\alpha_+^* \alpha_-](C(0_g^-, 2, 1) - C(0_g^+, 2, 1)), \\
A_{1,3} =\ & \Re[\alpha_+^* \alpha_0 - \alpha_0^* \alpha_-]C(1_g, 2, 3), \\
A_{2,3} =\ & \Im[\alpha_+^* \alpha_0 - \alpha_0^* \alpha_-]C(1_g, 2, 3), \\
A_{0,1} =\ & \Re[\alpha_+^* \alpha_0 + \alpha_0^* \alpha_-]C(1_g, 2, 3), \\
A_{0,2} =\ & \Im[\alpha_+^* \alpha_0 + \alpha_0^* \alpha_-]C(1_g, 2, 3), \\
A_{0,3} =\ & (|\alpha_+|^2 - |\alpha_-|^2)[C(2_g) - C(0_g^+, 2, 1)/2 \\
& - C(0_g^-, 2, 1)/2].
\end{aligned}
$$

The component $A_{0,0}$ weights a scalar energy shift which we ignore. The coefficients $C(|Y|_\sigma^\pm)$ quantify coupling to excited states with different symmetries and are given by

$$
\begin{aligned}
C(0_\sigma^m, j, k) =\ & K_j(0_\sigma^m)^2 s(0_\sigma^m(3/2)) + K_k(0_\sigma^m)^2 s(0_\sigma^m(1/2)), \\
C(1_\sigma, j, k) =\ & \sum_{a=1}^4 K_j^a({}^a 1_\sigma(3/2)) K_k^a({}^a 1_\sigma(3/2)) s({}^a 1_\sigma(3/2)) \\
& + \sum_{b=1}^2 K_j^b({}^b 1_\sigma(1/2)) K_k^b({}^b 1_\sigma(1/2)) s({}^b 1_\sigma(1/2)) \\
C(2_g) =\ & s(2_g(3/2)).
\end{aligned}
$$

Here the energy dependent terms $s(|Y|_\sigma^\pm(J)) = \hbar|\Omega|/[\hbar\omega_F - E(|Y|_\sigma^\pm(J))]$ quantify the amplitude in the excited states. The energies $E(|Y|_\sigma^\pm(J)))$ correspond to eigenvalues of H_{int} and the sets $\{K_j(0_\sigma^m(J))\}_{j=1}^2$ and $\{K_j^a({}^a 1_\sigma(J))\}_{j=1}^3$ are coefficients of the eigenvectors for $|Y| = 0, 1$. For $Y = 0$, the energies are $E(0_\sigma^+(1 \pm 1/2)) = 2B + \gamma[\sigma 3d^2/2\gamma r^3 - 1/4 \pm \sqrt{(\sigma d^2/2\gamma r^3 + 1/4)^2 + 1/2}]$, and $E(0_\sigma^-(1 \pm 1/2)) = 2B + \gamma[-\sigma d^2/2\gamma r^3 - 1/4 \pm \sqrt{(-\sigma 3d^2/2\gamma r^3 + 1/4)^2 + 1/2}]$, The eigenvector components are $K_1(0_\sigma^m) = \cos(\gamma_{O_\sigma^m}/2)$ and $K_2(0_\sigma^m) = \sin(\gamma_{O_\sigma^m}/2)$ where the angles satisfy $\tan(\gamma_{O_\sigma^+}) = \sqrt{2}/(1/2 + \sigma d^2/\gamma r^3)$, and $\tan(\gamma_{O_\sigma^-}) = \sqrt{2}/(1/2 - \sigma 3d^2/\gamma r^3)$. For $Y = \pm 1$ the eigenvectors and doubly degenerate eigenvalues are obtained by diagonalizing the 3×3 matrices:

$$
2B\mathbf{1}_3 + \frac{\gamma}{2}
\begin{pmatrix}
-\sigma\frac{2d^2}{\gamma r^3} & \pm 1 & \mp 1 \\
\pm 1 & -\sigma\frac{4d^2}{\gamma r^3} & 1 \\
\mp 1 & 1 & \sigma\frac{2d^2}{\gamma r^3}
\end{pmatrix}.
$$

For $Y = \pm 2$, the eigenvalues are doubly degenerate with energies $E(2_\sigma(3/2)) = 2B + \gamma/2 + \sigma d^2/r^3$.

A caveat is that we do not have point dipoles but rather wavepackets with spatial distributions parallel and perpendicular to the intermolecular axis $\hat{z}$. Components of intermolecular separations orthogonal to $\hat{z}$ will couple to states with different symmetry and an exact treatment would require averaging over the angular distrubution with the appropriate frame transformation. However, we argue that in our regime this finite size affect is negligible. The relative magnitude can be estimated by the ratio of the marginal relative coordinate probability distributions perpendicular and parallel to $\hat{z}$. Defining $p_\perp(r) = \int d\Omega \sin^2\theta r^2 |\psi_{\text{rel}}(r, \theta)|^2$ and $p_\parallel(r) = \int d\Omega \cos^2\theta r^2 |\psi_{\text{rel}}(r, \theta)|^2$, the peak of the distributions is at $r = \Delta z$ where for $z_0/\Delta z \ll 1$, the relative amount of unwanted couplings is $p_\perp(\Delta z)/p_\parallel(\Delta z) \sim 4(z_0/\Delta z)^2$. For molecular wavepacket localization $2\pi z_0/\lambda_{\text{trap}} = 0.1$, the ratio is $p_\perp(\lambda_{\text{trap}})/p_\parallel(\lambda_{\text{trap}}) \approx 10^{-3}$, hence it is warranted to compute the couplings as if the entire weight of the wavefunction were parallel to $\hat{z}$.

[1] M.A. Levin, and X.G. Wen, Phys. Rev. B **71**, 045110 (2005).
[2] M. Hermele, M.P.A. Fisher, and L. Balents, Phys. Rev. B **69**, 064404 (2004).
[3] T. Einarsson, Phys. Rev. Lett. **64**, 1995 (1984).
[4] D. Jaksch, and P. Zoller, Annals of Physics **315**, 52-79 (2005).
[5] H.P. Büchler, M. Hermele, S.D. Huber, M.P.A. Fisher, and P. Zoller, Phys. Rev. Lett. **95** , 040402 (2005).
[6] L. Santos, M.A. Baranov, J.I. Cirac, H.-U. Everts, H. Fehrmann, and M. Lewenstein, Phys. Rev. Lett. **93** 030601 (2004).
[7] *Special Issue on Ultracold Polar Molecules: Formation and Collisions*, Eur. Phys. J. D. **31** (2004).
[8] B. Duoçot, M.V. Feigel'man, L.B. Ioffe, and A.S.Ioselevich, Phys. Rev. B **71**, 024505 (2005).
[9] A.Yu. Kitaev, Preprint at <http://arxiv.org/abs/cond-mat/0506438> (2005).
[10] E. Dennis, A.Yu. Kitaev, A. Landahl, and J. Preskill, J. Math. Phys. **43**, 4452 (2002).
[11] L.M. Duan, E. Demler, and M.D. Lukin, Phys. Rev. Lett. **91**, 090402 (2003).
[12] J.M. Sage, S. Sainis, T.Bergeman, and D. DeMille, Phys. Rev.

Lett. **94** 203001 (2005).

[13] G.K. Brennen, I.H. Deutsch, and C.J. Williams, Phys. Rev. A **65**, 022313 (2002).

[14] S. Kotochigova, E. Tiesinga, and P.S. Julienne, Eur. Phys. J. D.

[15] M. Movre and G. Pichler, J.Phys. B: Atom. Molec. Phys. **10**, 2631 (1977).

31, 189 (2004).